Supplemental Materials

Molecular Biology of the Cell

Sullivan et al.

Influence of EGOC-foci on TORC1-body formation

To determine if TORC1 moves into the EGOC foci during body formation, we set out to follow EGOC and TORC1 localization in a single strain.

As a first step, we tagged Kog1 and all five EGOC subunits using mCherry and mRuby. These constructs all had very low signal. To overcome this problem, we tagged Kog1 with DuDre, a tandem array of DsRedExpress 2(Li et al., 2015). As expected,the Kog1-DuDre construct was brighter, making it possible to follow TORC1-body formation. However, after careful analysis we found that 30% of cells expressing Kog1-DuDre contain TORC1-bodies during log phase growth (3-fold higher than in Kog1-YFP and other previously studiedstrains)—indicating that the large tag on Kog1 disrupts interactions with EGOC and/or other inhibitors of TORC1-body formation. Nevertheless, we crossed the strainexpressing Kog1-DuDre with the strains carrying YFP-tagged EGO subunits, and found that TORC1-bodies co-localize with EGOC-fociduring both log growth and starvation (Fig. 2 and associated text)

To try and get around the problems associated withthe Kog1-DuDre construct, we nexttagged four out of the five EGOC subunits with DuDre. The Ego1-DuDre, Ego3-DuDre and Gtr1-DuDre constructs all had strong signals and were therefore crossed with a strain carrying Kog1-YFP. However, the resulting dual marker strains formed TORC1-bodies at a much lower rate than theparentalstrain expressing Kog1-YFP alone (Figs. 1 and S2). The resulting dual marker strains also formed far fewer EGOC-foci in log growth conditions than the constructs expressing EGOC-YFP alone, and in the case of Ego3, less than the construct tagged with Ego3-DuDre alone (Figs 2 and S2). Thus, theEGOC-DuDretags and Kog1-YFP tags clash/interfere with eachotherand disrupt EGOC-foci and TORC1-body formation. Again, however, when TORC1-bodies do form they co-localizewith EGOC–foci (Fig.S2).

Putting all the data together, it appears that EGOC-foci form before TORC1-bodies and may help to nucleate/accelerate TORC1-body formation. This model is supported by: (1) the data in Figs. 1 and 2 showing that EGOC-foci are formed in 60-70% of cells during log phase growth (before TORC1-bodies start to form), and that TORC1-bodies ultimately co-localize with the EGOC-foci. (2) The observation that mutants that disrupt EGOC-foci formation, but still carry Gtr1 and/or Gtr2, form TORC1-bodies slower than the wild-type strain (Figs. 1 and 2). (3) The observation that strains carrying Ego1-DuDre, Ego3-DuDre or Gtr1-DuDre with Kog1-YFP all have reduced levels of EGOC-foci formation in log growth conditions and also have a reduced rate of TORC1-body formation (Fig. S2). (4) The observation that EGOC-foci formation always precedes TORC1 body formation (Fig. 1, 2 and Fig. S2).

However, there are other models that could fit with the data described above. For example, EGOC-foci could dock onto the TORC1-body after it forms (in this case the low rate of TORC1-body formation in EGOC mutants would have to be explained by other mechanisms). Therefore, to confirm that TORC1-bodies assemble at the site of preformed EGOC-foci we attempted to follow Kog1 and EGOC localization over time in single cells. Unfortunately, due to the low signals from TORC1 and EGOC (and the resulting long exposure times needed to follow TORC1-body and EGOC-foci formation) there was too much photobleaching to follow TORC1 and EGOC localizationat multiple time-points in a single cell.

Properties of the Pib2 truncation mutants

The Pib2 truncation mutants were originally built and studied on plasmids(Michel et al., 2017). Thatwork showed that removal of the N-terminal domain of Pib2 (residues 1-164) conferred resistance to rapamycin (as expected if TORC1 is hyper-activated in the mutant) while removal of the extreme C-terminus of the protein (residues 620-635) causes sensitivity to rapamycin (as expected if TORC1 activity is repressed in the mutant). The original study also showed to that deletion of Pib2 limits TORC1 activation by glutamine (as measured by monitoring the phosphorylation of Sch9). However, the N-terminal truncation did not influence TORC1 activity in the Sch9 phosphorylation assay, and the authors did not measure the impact that other Pib2 truncations have on TORC1 activityusing the Sch9 assay.

In this work, we built each of the previously reported Pib2 truncation mutants (and some hybrids) at the native locusto ensure that the mutantproteins are expressed uniformly across the population of cells under study. To test if these constructs behave as expected, we first measured the sensitivity of each strain to rapamycin in the Kog1-YFP background. In line with the previous results, we found that deletion of the C-terminal domain conferred sensitivity to rapamycin (Fig. S4, upper panel) while deletion of the N-terminal domain confers resistance to rapamycin (Fig. S4, lower panels). Although we note that our *pib2*Δ strain is less sensitive to rapamycin than the strain studied by Michel et al (this may be due to differences in the base strain).

To further explore the impact that each domain in Pib2 has on TORC1 signaling, we measured TORC1 activity before and during nitrogen starvation in key truncation mutants. As expected, the *pib2*Δ strainhad significantly less TORC1 activity in rich medium (during log growth) than the wild-type strain (~75%of wild-type levels based on duplicate measurements; Fig. S5), but deletion of the N-terminal and C-terminal domains did not cause an appreciable change in TORC1 activity or repression by nitrogen starvation (Fig. S6).

Pib2 overexpression

Deletion of Pib2 blocks TORC1-body formation. To test if Pib2 overexpression speeds up TORC1-body formation we cloned full length Pib2, and GFP-Pib2, into a p415 plasmid containing a CYC1-promoter and introduced them into Kog1-YFP *pib2*Δ and *pib2*Δ strains, respectively. Pib2 expression from the plasmid was 2.6 ± 0.2-foldabove native levels (as measured by comparing the GFP-Pib2 signal from the native locus to that from the overexpression plasmid) --and covered for deletion of Pib2--but slowed TORC1-body formation (Fig. S6). This indicates that Pib2 levels are already sufficient in wild-typecellsto drive the maximum rate of TORC1-body formation and that excess Pib2 perturbs TORC1-body formation.

Li, D., Song, J.Z., Shan, M.H., Li, S.P., Liu, W., Li, H., Zhu, J., Wang, Y., Lin, J., and Xie, Z. (2015). A fluorescent tool set for yeast Atg proteins. Autophagy *11*, 954-960.

Michel, A.H., Hatakeyama, R., Kimmig, P., Arter, M., Peter, M., Matos, J., De Virgilio, C., and Kornmann, B. (2017). Functional mapping of yeast genomes by saturated transposition. Elife *6*.

Fig. S1. EGOC regulates TORC1-body formation in nitrogen starvation. Time-course data showing the fraction of cells containing Kog1-YFP puncta in the wild-type strain and strains missing Gtr1/2, or carrying a constitutively active Gtr1 allele (*Gtr1^{on}*), during nitrogen starvation (as labelled). Each time point shows the data from 90-180 cells, per time point. The solid lines show the best fit to a single exponential for the *gtr1*Δ*gtr2*Δ strain, a double exponential for the wild-type strain, and a straight line for the Gtr1^{on}strain, using the same rate constants found in glucose starvation.

Fig. S2. EGOC and TORC1 co-localization during starvation. Time-course data showing the fraction of cells containing EGOC puncta and/or TORC1-bodies during glucose starvation as measured in strains expressingKog1-YFP and Gtr1-DuDre, Ego1-DuDre or Ego3-DuDre (top, middle and bottom panels, respectively). The yellow points and lines show the percent of TORC1 bodies that co-localize with EGOC foci. Each time-point shows the average and standard deviation from three experiments, with 100-300 cells per time-point, per replicate. The grey points (on the y-axis) show the number of cells with EGOC foci in SD medium in cells carrying the relevant EGOC subunit tagged with DuDre, but no Kog1-YFP.

Fig. S3. Sch9 phosphorylation during glucose starvation. Western blots following Sch9 phosphorylation during glucose starvation in the wild-type strain, and mutant strains with severe defects in TORC1-body formation.

Fig. S4. Rapamycin sensitivity of Pib2 truncation mutants. The strains examined in Fig. 5 were spotted onto YEPD plates containing 0, 2 or 5 ng/ml rapamycin, with a five-fold dilution at each step.

Fig. S5+S6. Sch9 phosphorylation kinetics of Pib2 truncation mutants during nitrogen starvation. Western blots following Sch9 phosphorylation during nitrogen starvation in the wild-type strain, *npr2*Δ, and select Pib2 truncation mutants (Fig. 5). Experiments were performed and analyzed as described in Figs. 3d and e.

Fig. S7. Overexpression of Pib2 slows TORC1-body formation. Time-course data showing the fraction of cells containing Kog1-YFP puncta in the wild-type strain and strains missing Pib2, missing Pib2 and carrying an empty p415 plasmid (*pib2*Δ+ empty vector), or missing Pib2 and carrying a p415 plasmid with Pib2 under control of a CYC1 promoter (*pib2*Δ +Pib2OE).Each time-point shows the average and standard deviation from three experiments, with 100-300 cells per time-point, per replicate.

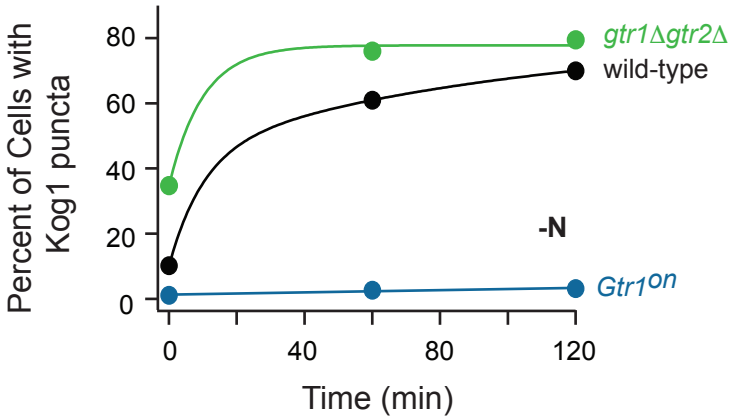
Percent of Cells with Kog1 puncta
80
60
40
20
0
0
40
80
120
Time (min)
gtr1Δgtr2Δ
wild-type
-N
Gtr1on

Fig. S1

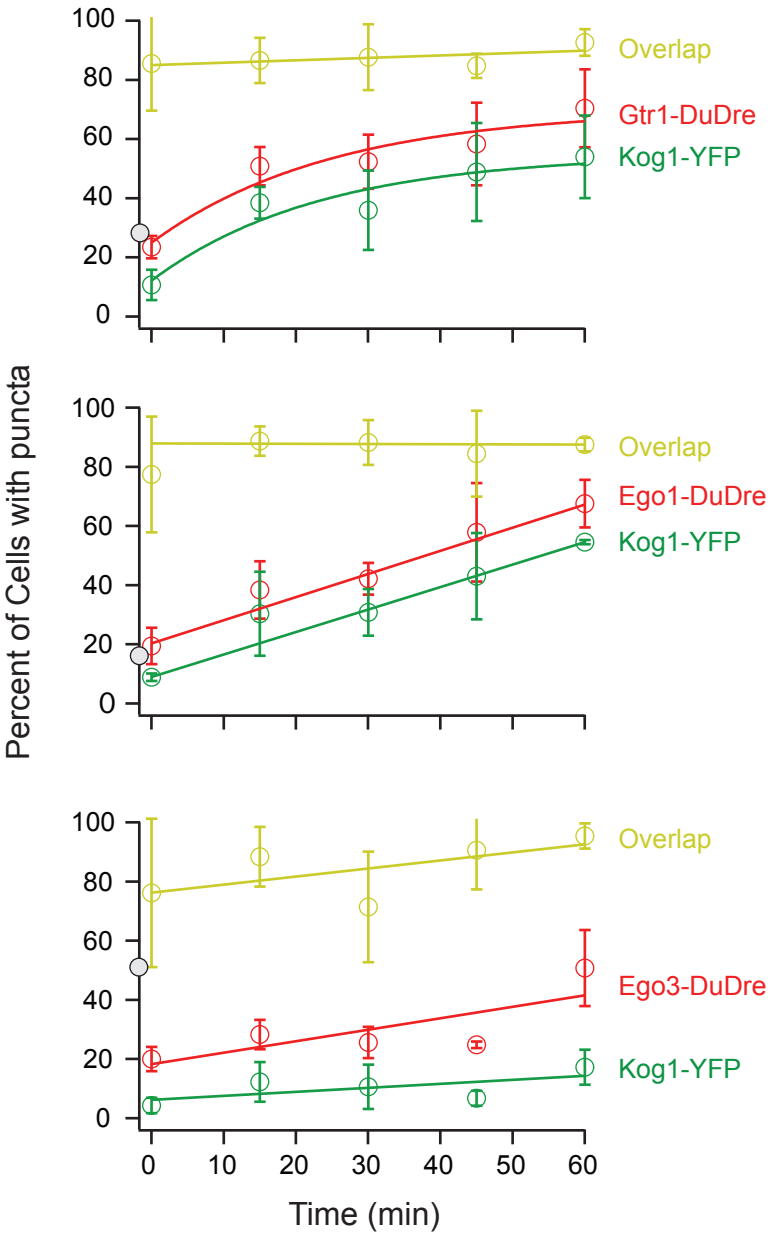
Percent of Cells with puncta
100
80
60
40
20
0
Overlap
Gtr1-DuDre
Kog1-YFP
Overlap
Ego1-DuDre
Kog1-YFP
Overlap
Ego3-DuDre
Kog1-YFP
0
10
20
30
40
50
60
Time (min)

Fig. S2

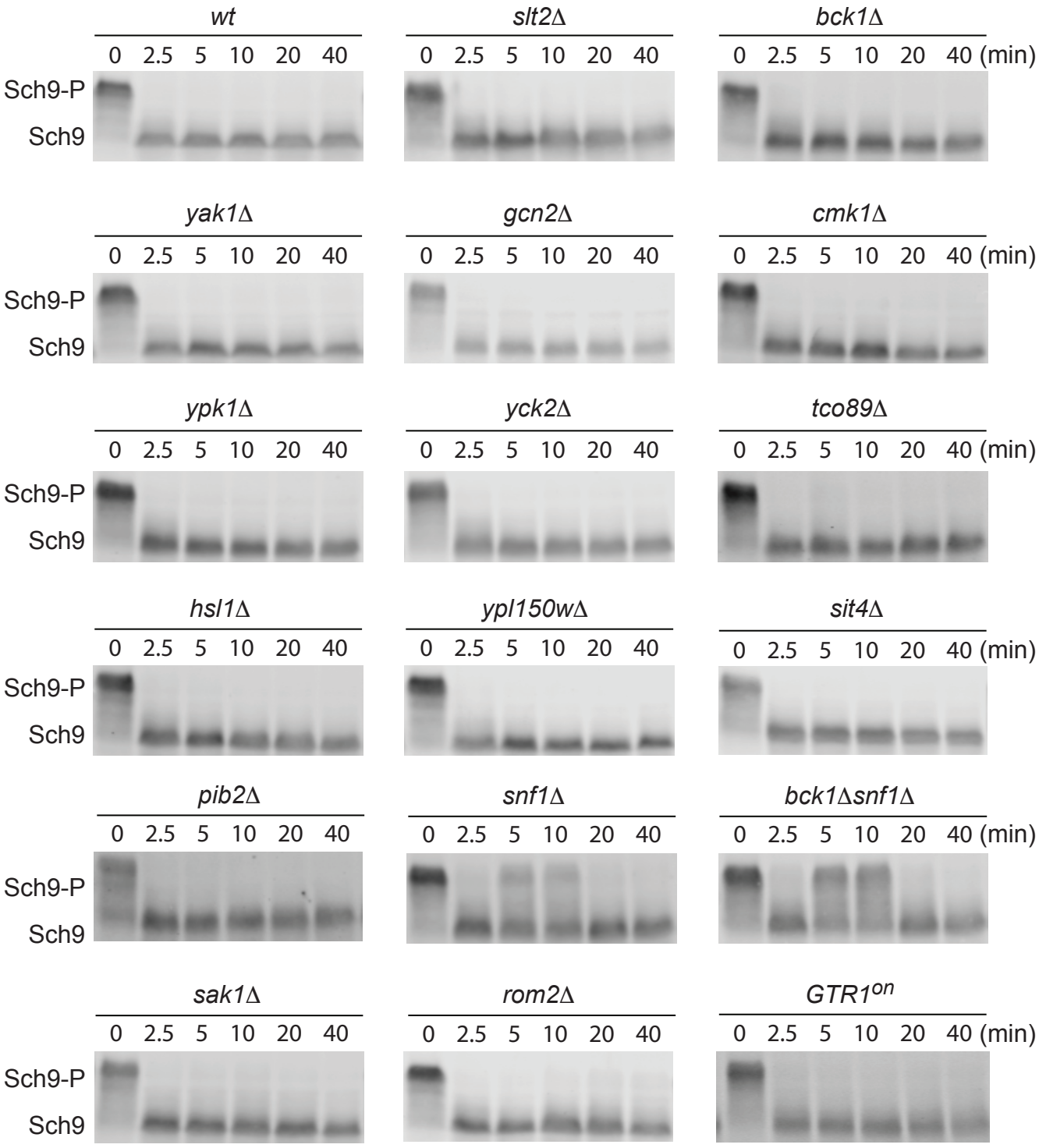
wt
slt2Δ
bck1Δ
yak1Δ
gcn2Δ
cmk1Δ
ypk1Δ
yck2Δ
tco89Δ
hsl1Δ
ypl150wΔ
sit4Δ
pib2Δ
snf1Δ
bck1Δsnf1Δ
sak1Δ
rom2Δ
GTR1on
0 2.5 5 10 20 40 (min)
Sch9-P
Sch9

Fig. S3

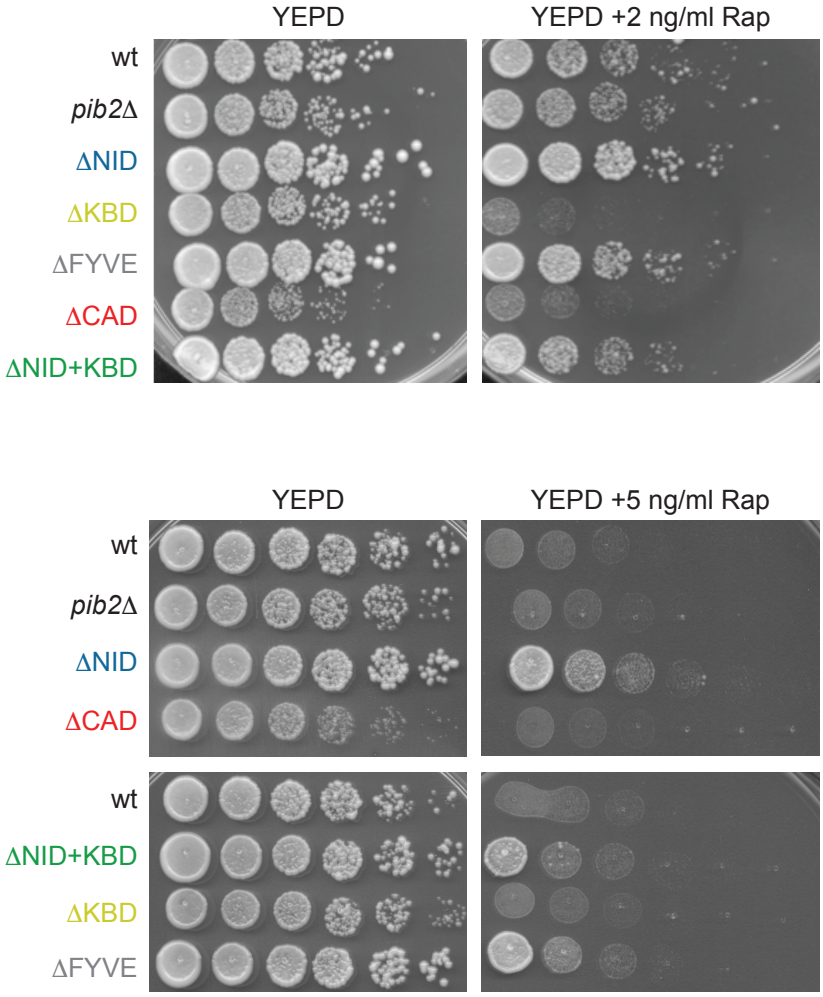
YEPD
YEPD +2 ng/ml Rap
wt
pib2Δ
ΔNID
ΔKBD
ΔFYVE
ΔCAD
ΔNID+KBD
YEPD
YEPD +5 ng/ml Rap
wt
pib2Δ
ΔNID
ΔCAD
wt
ΔNID+KBD
ΔKBD
ΔFYVE

Fig. S4

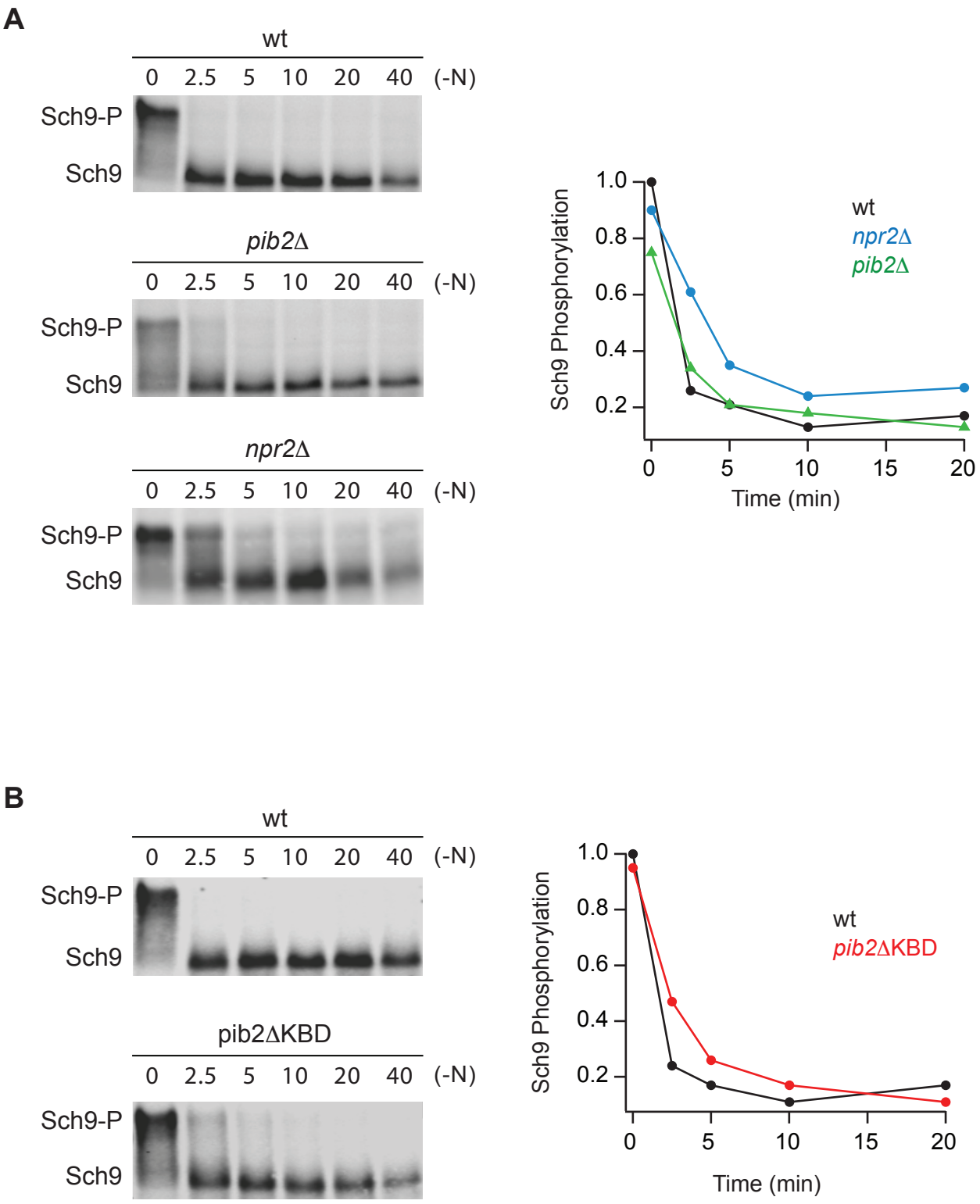
A
wt
0 2.5 5 10 20 40 (-N)
Sch9-P
Sch9
pib2Δ
0 2.5 5 10 20 40 (-N)
Sch9-P
Sch9
npr2Δ
0 2.5 5 10 20 40 (-N)
Sch9-P
Sch9
Sch9 Phosphorylation
1.0
0.8
0.6
0.4
0.2
0
5
10
15
20
Time (min)
wt
npr2Δ
pib2Δ
B
wt
0 2.5 5 10 20 40 (-N)
Sch9-P
Sch9
pib2ΔKBD
0 2.5 5 10 20 40 (-N)
Sch9-P
Sch9
Sch9 Phosphorylation
1.0
0.8
0.6
0.4
0.2
0
5
10
15
20
Time (min)
wt
pib2ΔKBD

Fig. S5

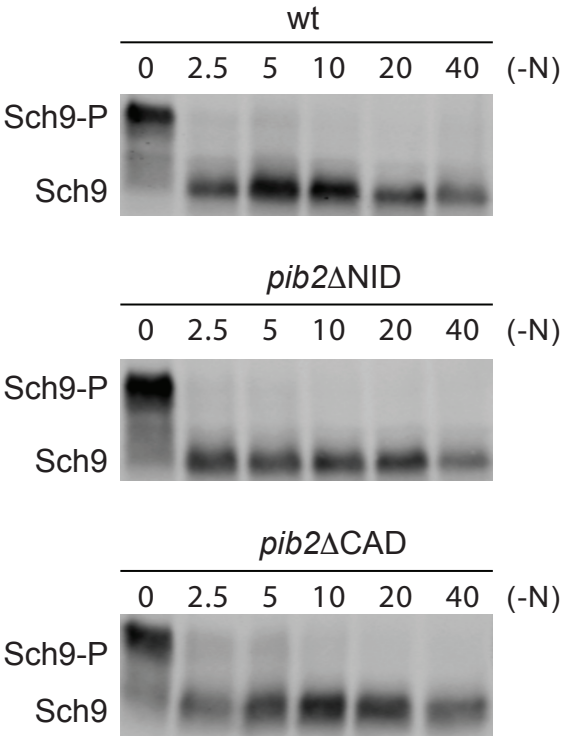
wt
0 2.5 5 10 20 40 (-N)
Sch9-P
Sch9
pib2ΔNID
0 2.5 5 10 20 40 (-N)
Sch9-P
Sch9
pib2ΔCAD
0 2.5 5 10 20 40 (-N)
Sch9-P
Sch9

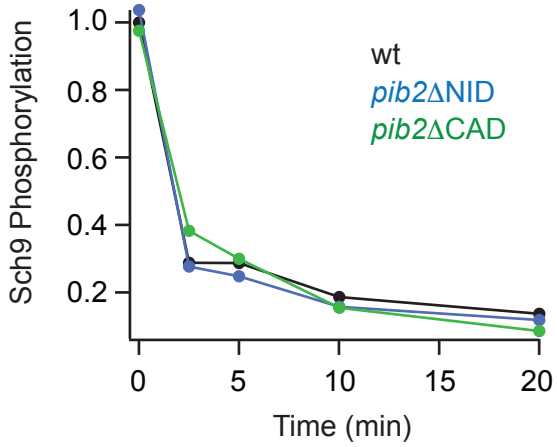
Sch9 Phosphorylation
1.0
0.8
0.6
0.4
0.2
0
5
10
15
20
Time (min)
wt
pib2ΔNID
pib2ΔCAD

Fig. S6

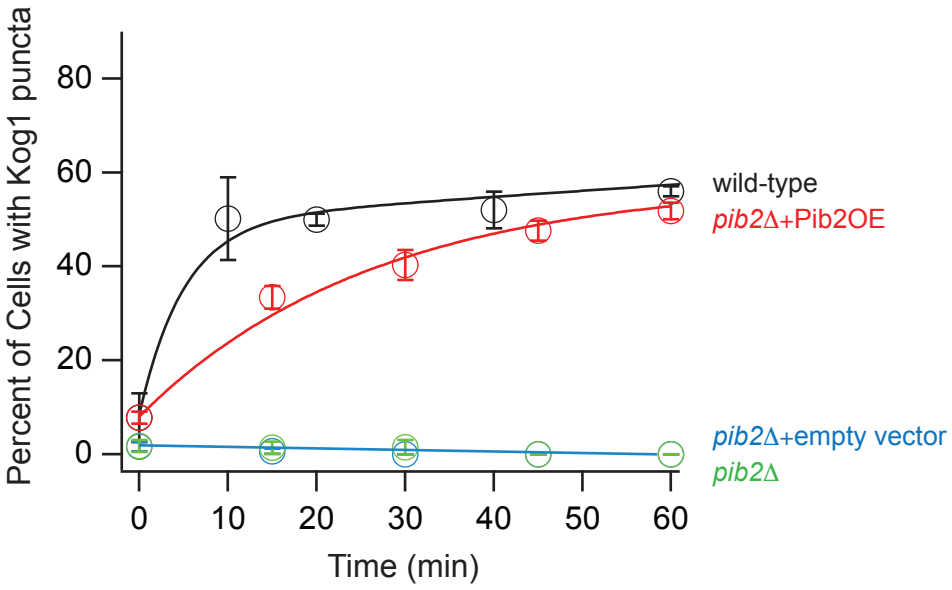
Percent of Cells with Kog1 puncta
80
60
40
20
0
0
10
20
30
40
50
60
Time (min)
wild-type
pib2Δ+Pib2OE
pib2Δ+empty vector
pib2Δ